

THE AUTOCATALYTIC DECOMPOSITION OF ACETIC ACID ON Ni(110)

R.J. MADIX^{*}, J.L. FALCONER and A.M. SUSZKO^{**}

*Department of Chemical Engineering,
Stanford University, Stanford, California 94305, U.S.A.*

Received 10 June 1975; manuscript received in final form 2 September 1975

The flash decomposition of CH_3COOH was studied on a clean nickel (110) surface following adsorption at 30°C in order to access the applicability of chemical reaction rate theory to a homologous series of reactants on a well-defined surface. As was observed for formic acid, acetic acid adsorbed at 30°C to yield gaseous H_2O and to form islands of adsorbed anhydride intermediates; the decomposition proceeded by a two-dimensional autocatalytic mechanism to form H_2 , CO_2 , Co and surface carbon. The decomposition of the anhydride was rate determining for the formation of CO_2 and H_2 . The rate of decomposition was well described by the equation governing the formic acid decomposition on the same surface. The activation energy for this first order decomposition was determined to be 28.2 kcal/gmol and the pre-exponential factor, ν , was found to be $6.4 \times 10^{14} \text{ s}^{-1}$ with a fraction of initiation sites of 0.004. These values were nearly the same as those observed for the decomposition of HCOOH , suggesting identical intramolecular mechanisms for the unimolecular decomposition of the adsorbed intermediates. The relative values of ν for the decomposition of HCOOH , DCOOH and CH_3COOH indicated that the motion of the H, D or CH_3 group was involved in the rate-limiting step.

1. Introduction

Although the catalytic decomposition of acetic acid has not been studied extensively, many studies exist for the simplest carboxylic acid, formic acid [1]. Recent studies revealed unique results for the decomposition of formic acid on clean Ni(110) [2–5]. The decomposition following adsorption of formic acid at room temperature proceeded autocatalytically, and rate constants for the elementary steps were accurately determined. The decomposition exhibited a large positive entropy of activation, yielding a preexponential factor of 1.6×10^{15} . The purpose of this study of the decomposition of acetic acid was to observe to what extent the qualitative characteristics

^{*} To whom correspondence should be addressed.

^{**} Work done in partial fulfillment of the Master of Science degree in Chemical Engineering at Stanford.

of the decomposition of the two simplest carboxylic acids were similar and to compare quantitatively the rate constants for the decomposition step.

The only reaction products observed for formic acid decomposition following adsorption of DCOOH on clean Ni(110) at -55°C were CO_2 , D_2 , CO and H_2O [5]. Adsorption at 37°C resulted in the immediate desorption of H_2O and the formation of a two-dimensional condensed phase composed of adsorbed intermediates believed to be formic anhydride. The autocatalytic nature of the decomposition was attributed to an increasing number of vacant sites within the condensed regions as products desorption occurred, the vacant sites acting as catalysts for the decomposition of the adsorbed molecules [4].

The shorthand notation previously discussed for product desorption was employed [4]. The notation $\text{A}(\alpha)/\text{B}(T)$ was used to denote desorption of the α state of gas A following adsorption of gas B at $T^{\circ}\text{C}$. Since most flash decomposition results in this paper were for a sample temperature of 30°C , the temperature notation was omitted in all discussion below except for adsorption at other temperatures.

2. Experimental

The flash desorption experiments were carried out in the stainless steel ultrahigh vacuum system previously described [2]. It contained a UTI quadrupole mass filter and four-grid LEED–AES optics. The (110)-oriented single crystal nickel sample was heated by radiation from a tungsten filament. Except where noted, a heating rate of 9.2 K s^{-1} was used. The sample could be cooled to -60°C within a few minutes by conduction from a liquid nitrogen cooled copper tube. Because of the system's high pumping speed the mass spectrometer signal during flash desorption was directly proportional to the desorption rate.

The nickel crystal was cleaned by bombardment with 300 V argon ions followed by annealing at 500°C until a clean Auger spectrum was obtained. Acetic acid was introduced onto the surface through a stainless steel dosing syringe directed at the front face of the crystal. Solid acetic acid at -45°C was used as the source for the dosing needle.

Reagent grade glacial acetic acid (Baker and Adamson, 98% purity) was employed after further purification by fractional recrystallization until a constant freezing point of 16.6°C was obtained [6]. The resulting acetic acid was vacuum distilled, and the middle half was collected and used for the dosing source. The final product was further purified by cycles of thawing, freezing and prolonged pumping at -45°C until a vapor pressure was obtained that did not vary with time. NMR analysis showed no detectable impurities, and the mass spectrometer cracking fraction, shown in fig. 1, showed the same cracking peaks obtained by others [7].

The acetic acid decomposition was studied under the same conditions reported for the formic acid decomposition [2,4]; because acetic acid decomposition resulted in the formation of a carbide residue on the surface the sample was either cleaned by

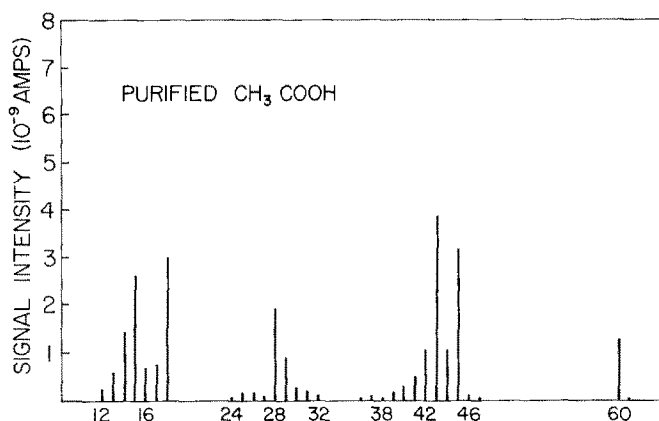


Fig. 1. The mass spectrum observed for acetic acid.

ion bombardment and annealed or simply heated to 700°C between each flash in order to maintain a clean surface [2]. The later procedure produced results characteristic of clean nickel up to about five flashes. Heating to only 500°C produced effects due to surface carbon after only one flash. At 700°C a carbidic surface is unstable with respect to a graphitic surface [12]. Reproducible flash desorption spectra were obtained for this surface; they were characteristic of clean Ni(110).

3. Results

3.1. CH_3COOH flash decomposition spectra

Acetic acid decomposition following adsorption at 30°C on clean Ni(110) yielded CO_2 , H_2 , CO and surface carbon when flashed to a final temperature of 500°C. A flash decomposition spectrum for CO_2 , H_2 and the signal at mass 28 is shown in fig. 2 for saturation coverage of CH_3COOH . The CO_2 and H_2 decomposition spectra each consisted of two peaks. The dominant CO_2 and H_2 peaks appeared at the same temperature with identical peak shapes. Carbon monoxide also desorbed in two peaks but the location and shape of these peaks was obscured by the presence of the CO^+ cracking fraction from CO_2 . No other flash desorption products were observed following adsorption at 30°C; in particular, CH_4 , C_2H_4 , and C_2H_6 were absent from the spectrum. The sticking probability for acetic acid appeared to be near unity, as was determined by comparison to the formic acid coverage versus exposure curves obtained for the same system.

Following CH_3COOH adsorption at -60°C, H_2O product peaks and an additional H_2 peak (see fig. 3) were observed. The additional H_2 peak was probably the result of adsorption from the background [5,8]. Water desorbed in a wide peak with a peak

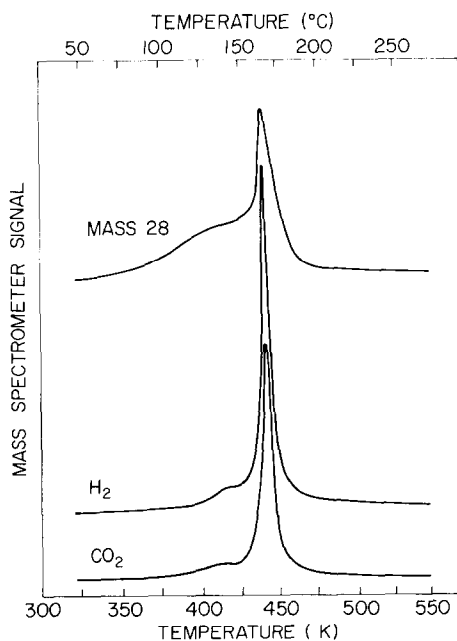


Fig. 2. Flash decomposition spectrum following adsorption of CH_3COOH to saturation coverage at 30°C .

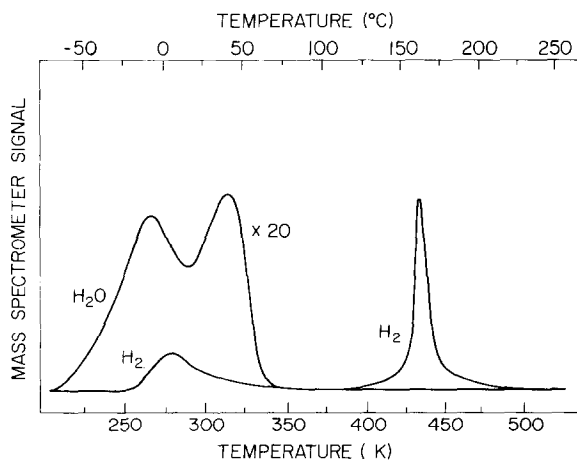


Fig. 3. H_2O and H_2 flash peaks observed following adsorption of CH_3COOH at -60°C .

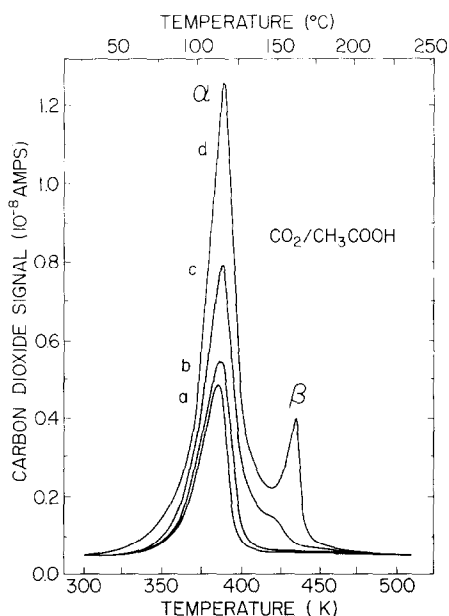


Fig. 4. Flash decomposition peaks for CO_2 following adsorption of CH_3COOH at 30°C ; low coverages. θ_{CO_2} = (a) 0.1, (b) 0.12, (c) 0.20, (d) 0.31.

temperature of 7°C at low coverage and two peaks at temperatures of -10°C and 41°C at high coverage. No other peaks were observed and unlike formic acid [2,5], the CO_2 , H_2 and CO peak shapes did not change significantly with adsorption temperature. Thus, the discussion of CO_2 , H_2 and CO evolution in this paper will be confined to adsorption at 30°C .

Carbon dioxide and hydrogen from CH_3COOH decomposition each desorbed in two peaks, a low temperature peak (α peak) and an extremely narrow peak at higher temperature (β peak). As shown in figs. 4 and 5 the $\text{CO}_2(\alpha)/\text{CH}_3\text{COOH}$ peak developed first with exposure to acetic acid; it was 21°C wide at half-maximum, and its peak temperature of 108°C was independent of coverage until the β peak emerged at higher coverage. The width of the β peak was 6°C , and its peak temperature was 165°C independent of coverage in the β -state for a ten-fold change in peak amplitude. As seen from figs. 2 and 6, the $\text{H}_2/\text{CH}_3\text{COOH}$ curves had the same shapes and locations as the CO_2 peaks. At the appearance of the β peak the α peak diminished in amplitude and shifted to higher temperatures. The behavior of the α and β peaks in the region of coverage in which the β peak emerged was complex and will not be discussed in detail.

The ratio of the areas of the flash curves for $\text{H}_2:\text{CO}_2$ and $\text{CO}:\text{CO}_2$ were constant to within 15% for coverages from 0.1 of saturation to saturation. Using the previously determined fact that the product ratio of $\text{H}_2:\text{CO}_2$ equalled unity for formic acid

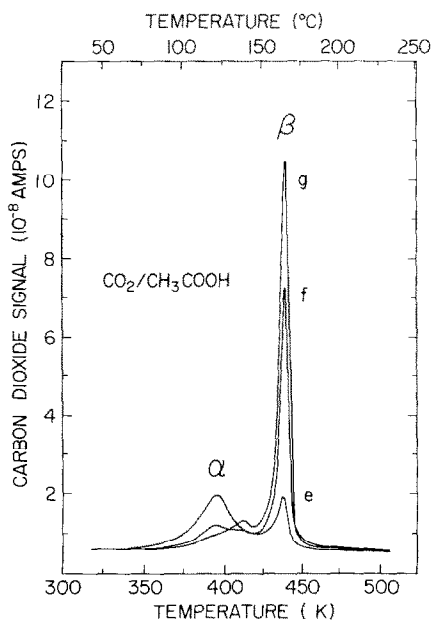


Fig. 5. Flash decomposition peaks for CO_2 following adsorption of CH_3COOH at 30°C ; high coverages. $\theta_{\text{CO}_2} = (\text{e}) 0.60, (\text{f}) 0.75, (\text{g}), 1.0$.

[2], the $\text{H}_2:\text{CO}_2$ ratio for acetic acid was found to be 3.0 ± 0.5 .

The flash decomposition spectra observed for mass 28 from the CH_3COOH decomposition was the superposition of a peak due to cracking from $\text{CO}_2(\alpha)/\text{CH}_3\text{COOH}$ and a peak corresponding exactly to $\text{CO}(\alpha_2)/\text{CO}$ and $\text{CO}(\alpha_2)/\text{DCOOH}$ [4]. At higher CH_3COOH coverages the $\text{CO}_2/\text{CH}_3\text{COOH}$ cracking peaks obscured separation of the CO peaks. The CO spectra obtained at high coverage after subtracting the mass spectrometer cracking fraction of CO_2 is shown as the dashed line in fig. 7. The spectrometer cracking fraction was calibrated by backfilling the chamber with CO_2 and recording the mass 44 and mass 28 signals as a function of CO_2 pressure. The slope of the mass 28 signal plotted against the mass 44 signal was the cracking fraction.

The $\text{CO}_2/\text{CH}_3\text{COOH}$ peak areas were compared to those obtained for CO_2/DCOOH (37) by decomposing CH_3COOH and DCOOH sequentially on the same surface. The $\text{CO}_2/\text{CH}_3\text{COOH}$ coverage following saturation of the surface with CH_3COOH was 0.9 ± 0.1 of the "saturation coverage" of CO_2/DCOOH . The saturation coverage of acetic acid was thus close to 2×10^{14} molecules/ cm^2 .

3.2. Activation energy determination

The activation energy for CH_3COOH decomposition to form the $\text{CO}_2(\beta)$ peak was determined by the method of heating rate variation [9]. Flash curves were obtained

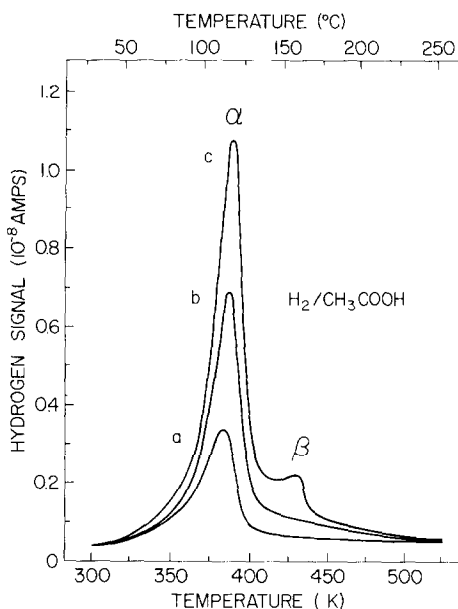


Fig. 6. Flash decomposition peaks for H_2 following adsorption of CH_3COOH at $30^\circ C$; low coverages.

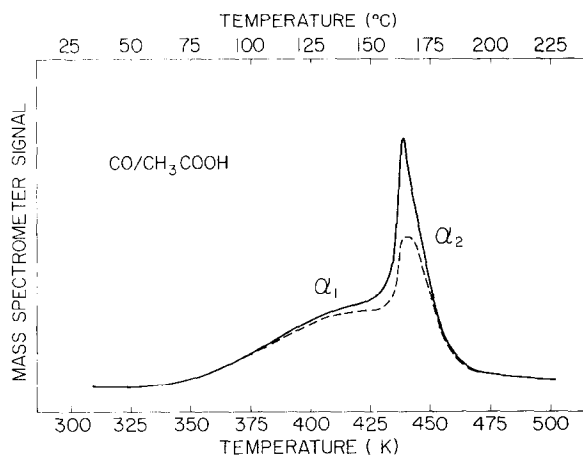


Fig. 7. Corrected CO flash desorption spectrum following CH_3COOH adsorption to high coverage at $30^\circ C$. The solid line is the experimental mass 28 data and the dashed curve results after subtracting the CO_2 cracking.

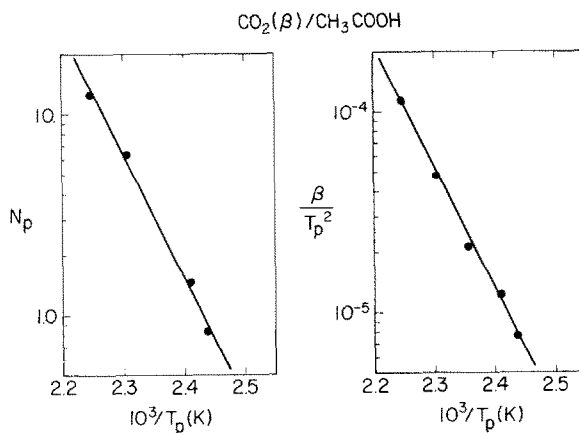


Fig. 8. Plots of (a) peak amplitude and (b) β/T_p^2 versus $10^3/T_p$ from heating rate variations.

for different heating rates between 1 K s^{-1} and 23 K s^{-1} for the same initial coverage of 0.8 saturation. The activation energy was determined without assuming pre-expo-

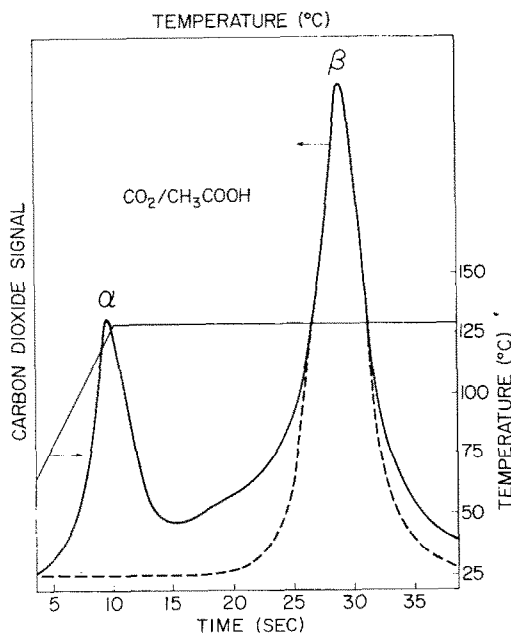


Fig. 9. Isothermal desorption rate for CO_2 with time showing the autocatalytic β peak. The solid curve shows the experimental data, and the dashed curve the calculated fit. The temperature–time curve is also shown.

nential factors, reaction mechanisms, or surface coverages by two methods. The $\log(\beta/T_p^2)$ was plotted versus $1/T_p$ in fig. 9, where β is the heating rate in K s^{-1} , and T_p is the peak temperature. Also $\log N_p$ was plotted versus $1/T_p$ as shown in fig. 8, where N_p is the peak amplitude in arbitrary units. Both plots were straight lines, and the least square fit yielded the same slopes for both lines corresponding to an activation energy of 28.2 kcal/mol.

3.3. Constant temperature desorption

Isothermal decomposition of DCOOH adsorbed on Ni(110) showed that the formic acid decomposed explosively on the clean surface [3,4]. The presence of a narrow $\text{CO}_2(\beta)/\text{CH}_3\text{COOH}$ peak indicated similar behavior for acetic acid adsorbed at 30°C. The CH_3COOH covered nickel was heated at 9.2 K s^{-1} to 129°C and held at that temperature, while the desorption rate of CO_2 was recorded as a function of time. Fig. 9 shows the $\text{CO}_2/\text{CH}_3\text{COOH}$ signal as a function of time for a saturated surface and the temperature time schedule employed. At 129°C the α peak had nearly desorbed, but the $\text{CO}_2(\beta)$ had not started to desorb. At constant temperature the desorption rate *increased with time* for the β peak, though the *surface coverage decreased*; i.e., the adsorbed acetic acid was decomposing autocatalytically on the clean surface.

3.4. The effect of surface carbon

A carbon peak was observed in the AES spectrum when the sample was flashed to only 500°C and cooled following acetic acid desorption. If this carbon peak was allowed to increase with subsequent acetic acid exposure, the flash decomposition spectra changed significantly. The resulting Auger spectrum taken after five successive flashes of approximately one-quarter monolayer of adsorbed acetic acid to 500°C showed a carbon coverage corresponding to one-third of a monolayer, and the fine structure of the carbon peak suggested bonding in the form of a carbide [10–12]. As the carbon coverage increased with exposure the $\text{CO}_2(\beta)/\text{CH}_3\text{COOH}$ peak shifted to higher temperatures, and its peak width increased. The α peak was not significantly affected by the carbon at these coverages.

4. Discussion

The flash decomposition of acetic acid on clean Ni(110) showed many similarities to formic acid decomposition on the same surface [4]. Both reactants yielded the same products, and the CO_2 and H_2 products desorbed in a narrow β peak the location of which did not change with initial coverage. In neither case could these narrow peaks be fit by a first-order desorption step for reasonable values of the rate constants. Also isothermal experiments showed the reactions to be the result of a kinetic ex-

plosion. Carbon dioxide and hydrogen also exhibited an α peak which developed at lower coverages and appeared at lower temperature than the β peak. The replacement of the carbon bound hydrogen atom in formic acid by a CH_3 group in acetic acid produced only secondary effects on the adsorbed state and the mechanism of decomposition though *the rate constant for decomposition to form CO_2 was reduced an order of magnitude*. The kinetic analysis developed for formic acid decomposition [4] applied equally well to the decomposition of acetic acid. Because extensive studies of CH_3COOH decomposition are not available, no comparison to studies in more conventional catalytic systems was possible.

4.1. Surface species and reaction stoichiometry

Flash decomposition of adsorbed acetic acid yielded CO_2 , H_2 and CO . The formation of $\text{CO}_2/\text{CH}_3\text{COOH}$ and $\text{H}_2/\text{CH}_3\text{COOH}$ was limited in rate by the decomposition of an adsorbed intermediate and not be the desorption of CO_2 or H_2 . This was determined by comparison to H_2/H_2 and CO_2/CO_2 spectra obtained previously [2]; H_2/H_2 desorbed with a peak temperature approximately 80 K lower than $\text{H}_2(\beta)/\text{CH}_3\text{COOH}$, and no CO_2/CO_2 desorption peaks were detected. Since $\text{CO}_2/\text{CH}_3\text{COOH}$ and $\text{H}_2/\text{CH}_3\text{COOH}$ desorbed at the same temperature with identical peak shapes, they were attributed to decomposition products from the same adsorbed intermediate.

The experimental results suggested that the reaction intermediate formed at high coverage was acetic anhydride. The evidence supporting this conclusion was the formation of a significant quantity of H_2O upon adsorption at -60°C , the ratio of $\text{H}_2:\text{CO}_2$ of three to one, the observance of only one dominant H_2 peak at high coverage, and the striking similarity to the decomposition of formic acid which was shown to evolve water from an intermolecular reaction involving only the acid hydrogens [5]. The adsorption of acetic acid at room temperature apparently produced a condensed phase of acetic anhydride and water which desorbed before flashing. Separate CH_3COO and CH_3CO fragments did not exist on the surface, since their decomposition to H_2 , CO_2 and CO would most certainly occur at different temperatures, yielding two distinct H_2 peaks of comparable magnitude. The observation of the formation of a surface anhydride following CH_3COOH adsorption, apparently without an activation energy lends more support to the postulate of formic anhydride on Ni(110). It is important to note that acetic anhydride is a stable gaseous molecule whereas formic anhydride is not.

At low coverages (below 0.3 of saturation) $\text{CO}/\text{CH}_3\text{COOH}$ corresponded exactly to $\text{CO}(\alpha_2)/\text{CO}$, so that decomposition to form CO at low coverage was desorption limited. At higher coverages the $\text{CO}_2(\beta)$ peak developed, and a second CO peak, the α_1 peak, also appeared (see fig. 8). The $\text{CO}(\alpha_1)/\text{CH}_3\text{COOH}$ peak was formed at the same temperatures as $\text{CO}_2(\alpha)/\text{CH}_3\text{COOH}$, and the $\text{CO}(\alpha_2)/\text{CH}_3\text{COOH}$ peak desorbed at the same temperatures as $\text{CO}_2(\beta)/\text{CH}_3\text{COOH}$. Thus quantitative separation of the CO_2 cracking fraction from the CO peaks was difficult. It appears, however, that $\text{CO}(\alpha_1)/\text{CH}_3\text{COOH}$ was the result of direct decomposition of the adsorbed anhydride

intermediate. This result suggests that at high surface coverage some CO desorbed from the surface due to the unavailability of binding sites for CO. At low coverages apparently all the CO formed from decomposition filled the $\text{CO}(\alpha_2)$ sites. This feature of the decomposition was not readily apparent from the HCOOH study.

4.2. Kinetics of decomposition

The kinetics of the acetic acid decomposition on clean Ni(110) was qualitatively identical to that for DCOOH decomposition and will not be discussed in detail here [4]. The characteristic β peaks were formed as islands of tightly packed acetic anhydride molecules decomposed via interaction with vacant metal sites. In analogy to DCOOH decomposition initial exposure of the Ni(110) surface to acetic acid resulted in the filling of a small number of initiation sites and populated the surface with additional, rather widely dispersed, anhydride species. As the surface coverage increased the adsorbing species began to condense into islands as evidenced by the appearance of $\text{CO}_2(\beta)$ peaks. With the formation of islands, regions of adsorbed species of both high and low density existed. The decomposition of the low density regions resulted in the α peaks; and the decomposition of the high density regions resulted in the β peaks. The β -state decomposition was slower than the α -state decomposition. This was attributed to the small concentration of bare metal sites in the high density islands. As product desorption yielded vacant sites in the islands, reaction at these sites occurred to create more vacant sites, and an accelerating rate of surface explosion was established.

The activation energy for the autocatalytic decomposition was determined to be 28.2 kcal/mol from heating rate variation, and the value of f was taken to be 0.004, the same as that for formic acid decomposition on Ni(110). The preexponential factor required to yield the correct peak temperatures and shape was $6.4 \times 10^{14} \text{ s}^{-1}$. The flash curve calculated from these values for $\text{CO}_2(\beta)/\text{CH}_3\text{COOH}$ is shown as a dashed line in fig. 10. The calculated and observed curves were coincident throughout most of the β peak. On the extreme high temperature side the experimentally observed rate was higher than the calculated value; on the leading edge of the β peak interference from the α peak made exact comparison difficult. Eq. (2) was also integrated numerically as a function of time for constant k to calculate isothermal desorption curves. The calculated curve normalized to the experimental peak amplitude is shown as a dashed line in fig. 9. Agreement between experiment and theory was very good.

A theoretical $\text{CO}_2(\alpha)/\text{CH}_3\text{COOH}$ peak was calculated by assuming that the α peak arose from a dilute adsorbed phase with a decomposition rate given by eq. (1) using the same rate constant evaluated for the β peak. The calculated curve is shown as a dashed line in fig. 10; it did not fit the experimental α peak very well.

Apparently the first-order α peak did not correspond simply to decomposition in a dilute region with rate parameters identical to the β state. The $\text{CO}_2(\alpha)$ peak was fit empirically at low coverages using approximate values of ν and E obtained from the

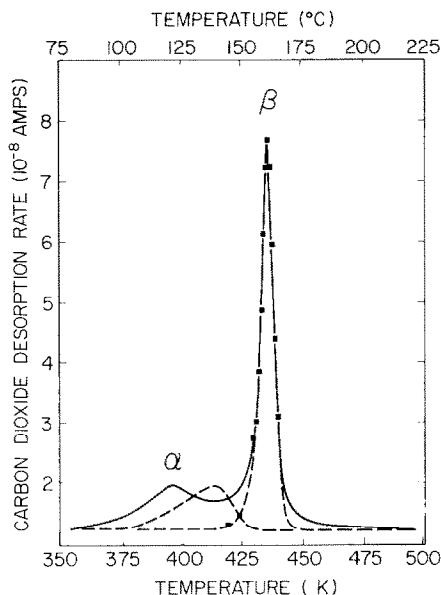


Fig. 10. The calculated $\text{CO}_2(\alpha, \beta)/\text{CH}_3\text{COOH}$ curve (dashed) from eqs. (2) and (4) versus the experimental curve (solid).

peak width and peak temperature [13]. These values were then adjusted so that numerical integration of eq. (4) yielded the experimental peak temperature and peak width. The resulting values for E and ν were 31 kcal/mol and $4.3 \times 10^{17} \text{ s}^{-1}$. The flash desorption curve calculated from these values is shown in fig. 11 with its amplitude normalized to the experimental curve. The agreement was good. The larger values of E and ν indicate that the $\text{CO}_2(\alpha)/\text{CH}_3\text{COOH}$ peak was the result of a different nature than that giving rise to the β peak.

4.3. Elementary reaction steps

The proposed mechanism and the flash decomposition results indicated excellent agreement with that found for the DCOOH decomposition [4]. It should be noted that even at saturation every adsorbed acetic acid molecule occupied four to five nickel surface atoms, and the actual number of surface atoms participating in each elementary step was not known. The magnitude of the pre-exponential factor for the rate-determining step indicated a large positive entropy change in passing from the adsorbed intermediate to the transition state. If CO was presumed to adsorb in the decomposition of the anhydride the only appreciable entropy gain in the transition state available was 13.9 cal/deg mol due to rotational motion of the CO_2 formed. It seems most likely that the transition state necessitated a nearly free CO_2 molecule;

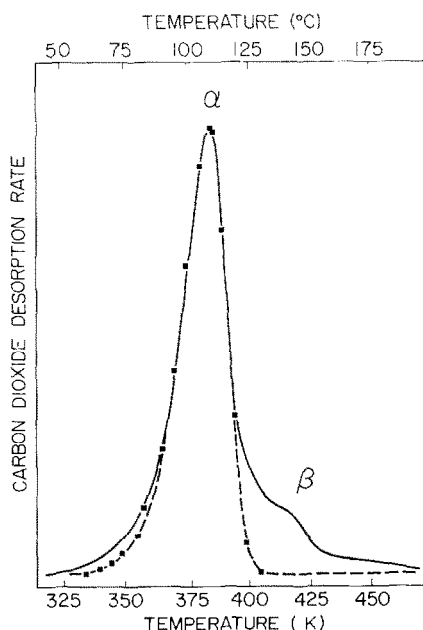
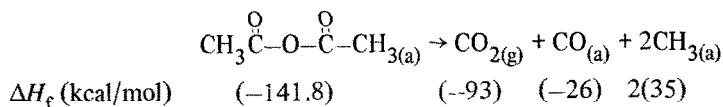


Fig. 11. Calculated first-order $\text{CO}_2(\alpha)/\text{CH}_3\text{COOH}$ curve (dashed) versus experimental curve (solid) for $E = 31 \text{ kcal/mol}$ and $\nu = 4.3 \times 10^{17} \text{ s}^{-1}$.

i.e., the transition state resided very near the products. Furthermore, the nearly identical values of the Arrhenius parameters for both the decomposition of formic acid and acetic acid on Ni(110) [4] suggest that the reaction coordinate in the two cases was identical. The common feature in these two cases is of course the $\begin{array}{c} \text{O} \quad \text{O} \\ \parallel \quad \parallel \\ -\text{C}-\text{O}-\text{C}- \end{array}$ group.

The rate-determining step cannot be more endothermic than the observed activation energy of 28.2 kcal/mol. If [14,15]



is taken to be the actual rate-determining step, its endothermicity can be estimated from the heats of formation of reactants and products listed, provided the binding energies of the adsorbed species can be estimated. The binding energy for CO on Ni(110) is 32 kcal/mol [9,16,17] and the heat of dissociative adsorption of H_2 on Ni(110) is 22 kcal/mol [2,18]. If the relative binding energies of $\text{CH}_{3(a)}$ and $\text{H}_{(a)}$ to the Ni(110) surface were taken to be the same as the relative H—C and C—C single bond energies, the exothermicity of the above reaction was calculated to be approximately 50 kcal/mol, taking the heat of adsorption of the acetic anhydride to be zero.

As the overall reaction can be 28 kcal/mol endothermic without contradicting the observed activation energy, the anhydride intermediate could be bound to the surface as strongly as 78 kcal/mol. Since the transition state appears to lie close to the products, it seems likely that the anhydride intermediate is very strongly bound to the surface. Finally, it is interesting to note that the ratio of preexponential factors for HCOOH , DCOOH and CH_3COOH scale closely as the square root of the mass ratios of the carbon-bound groups H, D and CH_3 . This is suggestive that the normal mode of vibration which represents the reaction coordinate involves the extension of the R—C bond. Due to the difficulty in assigning a precise surface structure of the adsorbed intermediate and the transition state, little more can be said on this point at this time.

5. Summary

The flash decomposition of acetic acid on Ni(110) following adsorption at 30°C was analogous to that observed for formic acid. Upon adsorption a surface anhydride intermediate was formed without activation energy; H_2 and CO_2 were formed in a single rate-limiting step, and CO was evolved by desorption-limited process. The stability of the surface anhydride indicated that the hydrogens on the methyl groups did not detach and adsorb as hydrogen atoms on the surface; the methyl groups apparently interact weakly with the surface. The high entropy of activation for the decomposition indicated a transition state very near the products. The bonding energy of the anhydride intermediate to the surface was estimated to be at least 50 kcal/mol.

Acknowledgements

The authors gratefully acknowledge the National Science Foundation and the Center for Materials Research at Stanford for financial support of this research. Acknowledgement is also made to the Donors of The Petroleum Research Fund, administered by the American Chemical Society, for partial support of this research.

References

- [1] P. Mars, J.J.F. Scholten and P. Zwietering, *Advan. Catalysis* 14 (1963) 35.
- [2] J. McCarty, J. Falconer and R.J. Madix, *J. Catalysis* 30 (1973) 235.
- [3] J.L. Falconer, J.G. McCarty and R.J. Madix, *Surface Sci.* 42 (1974) 329.
- [4] J.L. Falconer and R.J. Madix, *Surface Sci.* 46 (1974) 473.
- [5] J.L. Falconer and R.J. Madix, to be published.
- [6] *Handbook of Chemistry and Physics* (Chemical Rubber Co., Cleveland, Ohio, 1973).
- [7] *Atlas of Mass Spectral Data*, Vol. 1, Eds. E. Stenhagen, S. Abrahamson and F.W. McLafferty (Interscience, New York, 1969) p. 37.

- [8] G. Ertl and D. Kupperts, Ber. Bunsenges Phys. Chem. 75 (1971) 1017.
- [9] J.L. Falconer and R.J. Madix, Surface Sci. 48 (1975) 393.
- [10] R.J. Madix, J. Falconer and J. McCarty, J. Catalysis 31 (1973) 316.
- [11] T.W. Haas, J.T. Grant and G.J. Dooley III, in: Adsorption–Desorption Phenomena, Ed. F. Ricca (Academic Press, New York, 1972).
- [12] J.G. McCarty and R.J. Madix, to be published.
- [13] L.D. Schmidt, Catal. Rev. Sci. Eng. 9 (1974) 115.
- [14] S.W. Benson and H.E. O'Neal, Kinetic Data on Gas Phase Unimolecular Reactions (National Bureau of Standards 21, Feb. 1970).
- [15] JANAF Thermochemical Tables, 2nd ed. (National Bureau of Standards 31, June 1971).
- [16] T.N. Taylor and P.J. Estrup, J. Vacuum Sci. Technol. 10 (1973) 26.
- [17] H.H. Madden, T. Kupperts and G. Ertl, J. Chem. Phys. 58 (1973) 3401.
- [18] J. Lapujoulade and K.S. Neil, Compt. Rend. (Paris) 274 (1972) 2125.